# Gypenosides Protect Orbital Fibroblasts in Graves Ophthalmopathy via Anti-Inflammation and Anti-Fibrosis Effects

Haoyu Li, Chao Ma, Wei Liu, Jianfeng He, and Kaijun Li

Department of Ophthalmology, the First Affiliated Hospital of Guangxi Medical University, Guangxi, China

Correspondence: Kaijun Li, Department of Ophthalmology, the First Affiliated Hospital of Guangxi Medical University, 6 Shuangyong Road, Nanning, 530021 Guangxi Zhuang Autonomous Region, China; lkj_0285@qq.com.

HL and CM contributed equally to this work.

**Received:** September 30, 2019
**Accepted:** April 17, 2020
**Published:** May 27, 2020

Citation: Li H, Ma C, Liu W, He J, Li K. Gypenosides protect orbital fibroblasts in Graves ophthalmopathy via anti-inflammation and anti-fibrosis effects. *Invest Ophthalmol Vis Sci.* 2020;61(5):64. https://doi.org/10.1167/iovs.61.5.64

**Purpose.** To investigate the effect of Gypenosides (Gyps) on the inflammation and fibrosis in orbital fibroblasts (OFs) in Graves ophthalmopathy (GO).

**Methods.** Bioinformatics analyses were performed to identify the enriched genes and signaling pathways related to Gyps function. For ex vivo experiments, OFs were cultured from orbital connective tissues from patients with GO. OF proliferation was estimated by Cell Counting Kit-8 assay. Effects of Gyps treatment on interleukin (IL)-1$\beta$-induced inflammation and transforming growth factor-$\beta$1 (TGF-$\beta$1)-induced fibrosis were evaluated by real-time quantitative PCR (RT-qPCR), enzyme-linked immunosorbent assay (ELISA), and Western blotting. OFs were treated with IL-1$\beta$ or TGF-$\beta$1 in the absence or presence of Gyps pretreatment, and the levels of related mRNA or proteins were evaluated by RT-qPCR or ELISA.

**Results.** Eight inflammation-related target genes and nine fibrosis-related target genes were screened out. These genes were mainly enriched in pathways corresponding to inflammation and fibrosis, respectively. IL-1$\beta$-induced upregulation of inflammatory cytokines, and TGF-$\beta$-induced upregulation of fibrotic mediators in OFs were downregulated by Gyps. Moreover, Gyps reduced the activation of Toll like receptors 4/nuclear factor-$\kappa$ B signaling and TGF-$\beta$1/SMAD2/SMAD4 signaling in GO OFs.

**Conclusions.** Gyps could protect GO-derived OFs against IL-1$\beta$-induced inflammation and TGF-$\beta$1-induced fibrosis. Thus Gyps might have therapeutic potential on inflammation and fibrosis in GO.

Keywords: orbital fibroblast, Graves ophthalmopathy, inflammation, fibrosis

Graves ophthalmopathy (GO) is the most common orbital disease in adults.[1] Ocular lesions are caused by the enlargement of extraocular muscles and periorbital soft tissues because of the activation of connective tissues.[2] The symptoms of GO include upper eyelid retraction, edema, periorbital erythema, eyeball protrusion, and other manifestations. Some patients have a self-limiting course of disease, whereas approximately 5% to 15% of patients cannot recover.[3] These patients may develop to exposed keratitis, corneal ulcer, or optic neuropathy, thus affecting the patients' appearance and vision even leading to blindness.[4]

However, there are still many shortcomings in current treatment methods. Glucocorticoid therapy has anti-inflammatory and immunosuppressive effects, but requires a large dosage for long periods that may lead to several hormonal complications, such as hyperglycemia, elevated blood pressure, and liver failure.[5] In addition, a small number of patients with severe GO are insensitive to hormonal therapy. The orbital decompression surgery is invasive and needs high technical equipment with a long learning time. These disadvantages lead to different surgical methods and effects. Besides, orbital radiotherapy has been less carried out in many countries, including China. Hence it is urgent to develop new effective treatment methods to improve the prognosis of patients with severe GO.

According to the pathological changes of GO, the development of corresponding targeted therapies is an important research topic. Previous studies have shown that orbital fibroblasts (OFs) are affected by inflammatory mediators secreted by inflammatory cells, such as T cells, B cells, macrophages, and mast cells.[6,7] Additionally, OFs can express surface receptors, such as thyroid stimulating hormone receptor (TSHR) and insulin-like growth factor 1 receptor (IGF-1R), which mediate pathological processes of GO by regulating cell proliferation, inflammatory factor secretion, extracellular matrix synthesis, or fibrosis.[8] OFs participate in immune modulating, fibrosis, and oxidation, which are important factors for the initiation and development of GO, and are also major targets for the development of GO treatment strategies.

Many studies regarding GO have shown that IL-1$\beta$ can stimulate OFs to secrete cytokines, such as interleukin (IL)-6, IL-8, tumor necrosis factor-$\alpha$ (TNF-$\alpha$), monocyte chemoattractant protein-1 (MCP-1), prostaglandin E2, and other factors via activating nuclear factor-$\kappa$ B (NF-$\kappa$B) signaling pathway.[9,10] Moreover, Toll-like receptors (TLRs) activate the translocation of NF-$\kappa$B through the intracellular signal trans-

Table 1. Clinical Information of the Patients Included in this Study

| Age (y) | Sex | Smoker | BMI | Duration of GO (years) | CAS | Proptosis R/L (mm) | Surgical treatment |
|---|---|---|---|---|---|---|---|
| Patients with GO | | | | | | | |
| 61 | Female | N | 22.8 | 0.5 | 0/7 | 21/20 | Decompression |
| 48 | Female | N | 22.9 | 0.5 | 1/7 | 20/22 | Decompression |
| 52 | Female | N | 25.8 | 1 | 1/7 | 19/21 | Decompression |
| 49 | Male | Y | 20.3 | 1 | 3/7 | 20/18 | Decompression |
| 57 | Male | N | 19.5 | 20 | 1/7 | 23/23 | Decompression |
| 63 | Male | N | 22.8 | 0.6 | 1/7 | 21/19 | Decompression |
| Non-GO control subjects | | | | | | | |
| 35 | Female | N | 22.6 | n/a | n/a | n/a | Eye evisceration |
| 21 | Male | N | 23.6 | n/a | n/a | n/a | Eye evisceration |
| 50 | Male | Y | 23.9 | n/a | n/a | n/a | Eye evisceration |
| 33 | Female | N | 21.3 | n/a | n/a | n/a | Upper lid blepharoplasty |

BMI, body mass index; CAS, clinical activity score; n/a, not applicable; N, no; R, right eye; L, left eye; Y, yes.

duction of the downstream signaling molecule, thus leading to the production of TNF-$\alpha$ and other inflammatory cytokines.[11] These cytokines then recruit and activate T cells, B cells, monocytes, and mast cells to aggravate inflammatory response in the orbital tissue. In addition, fibrosis is one of the ultimate results of chronic inflammation. A previous study indicated that transforming growth factor-$\beta$1 (TGF-$\beta$1) can induce the transformation of OFs into myofibroblasts, promote the synthesis of extracellular matrix, and aggravate the fibrosis of extraocular muscles.[12] Some evidence has also proved that TGF-$\beta$/SMAD pathway is involved in the process of fibrosis in liver, lung, and kidney.[13,14]

Gypenosides (Gyps), which are saponins extracted from the *Gynostemma pentaphyllum*, represent the most pharmacologically active components in *G. pentaphyllum* and have several bioactivities. For example, Gyps can regulate the activation of immune cells and the expression of cytokines.[15] Gyps have been reported to regulate NF-$\kappa$B signaling pathway and inhibit IL-1$\beta$-induced inflammatory response in human osteoarthritic chondrocytes.[16] Additionally, Gyps can decrease inflammatory response in inflammatory bowel disease by inhibiting NF-$\kappa$B and signal transducer and activator of transcription 3 (STAT3) signal pathways.[17] Moreover, Gyps can reduce hepatic fibrosis by inhibiting the expression of TGF-$\beta$1, TGF-$\beta$1 receptor 1, SMAD family member 2 (SMAD2), and SMAD family member 3 (SMAD3); thus reducing the differentiation of hepatic progenitor cells into myofibroblasts.[18,19] Thus Gyps may serve as potential therapeutic targets in GOs orbit inflammatory infiltration and fibrotic proliferation. In this study, we studied the effects of Gyps on OFs derived from GO patients.

## Methods

### Target Collecting and Bioinformatics Analysis

Literature regarding the therapeutic mechanisms of Gyps were screened. Gene targets working on inflammation and fibrosis were identified according to the previous studies. Gene ontology, Kyoto encyclopedia of genes and genomes (KEGG), and Reactome pathway analyses could provide gene expression data for identified genes. Based on these earlier mentioned hub target genes, gene ontology and KEGG analyses were performed to clarify the mechanisms employed by Gyps for treating inflammation and fibrosis using the Database for Annotation, Visualization and Integrated Discovery (DAVID) v6.8 (https://david.ncifcrf.gov/)[20,21] and STRING v11.0 (https://string-db.org/).

### Cell Culture

Orbital connective tissues were collected from GO patients with dysthyroid optic neuropathy during orbital decompression surgery (clinical activity scores at the time of surgery were <4). Normal control tissues were harvested during evisceration or upper lid blepharoplasty from patients without history or clinical evidence of any thyroid disease. The characteristics of patients included in this study are shown in Table 1. Because of the limited number of donors, it was difficult to achieve perfect matching of the clinical characteristics of GO and non-GO patients. The institutional review board of the First Affiliated Hospital of Guangxi Medical University, Nanning, China, approved the study, and informed consent was obtained from all participants. This study followed the tenets of the Declaration of Helsinki. Tissues were used for the primary culture of human OFs. Each tissue was minced into pieces approximately 1×1 mm in size, placed in 35-mm plastic culture plates in Dulbecco's Modified Eagle Medium (DMEM) with antibiotics, and 20% fetal bovine serum (FBS), and incubated at 37°C in a humidified incubator under 5% $CO_2$ and 95% air at one atmosphere. Medium was changed three times per week. On reaching confluence, the medium was removed, and the cells were washed twice with phosphate buffered saline (PBS). Then cells were trypsinized with 0.25% trypsin/ethylenediaminetetraacetic acid solution and subcultured in 25 $cm^2$ plastic cell culture flasks in DMEM with antibiotics and 10% FBS. Gyps and IL-1$\beta$/TGF-$\beta$1 for cell culture were purchased from Jiatian Biotechnology (Xi'an, China) and Pepro Technology (NJ, USA), respectively. Cells between the second and eighth passages were used for the following experiments.

### Immunohistology

To identify different cell types, immunohistology was performed. Cells on the slides were fixed with 4% paraformaldehyde for 20 minutes at room temperature, followed by permeabilization with 0.05% Triton X-100 for 15 minutes at 4°C, and then blocked with PBS containing 4% BSA (Dalian Meilun Biotechnology, Dalian, China) for 30 minutes at 37°C. Primary antibodies were incubated overnight at 4°C with rabbit anti-S100 calcium binding protein B (S100B), rabbit anti-myoglobin (MB), rabbit anti-desmin (DES), rabbit anti-keratin 17 (KRT17), or rabbit anti-vimentin (VIM) antibodies (Sangon Biotech, Shanghai, China), and then incubated with biotin goat-antirabbit

Investigative Ophthalmology & Visual Science

IgG (Histostain-Plus Kits; Bioss, Beijing, China) for 1 hour at room temperature. Endogenous peroxidase activity was inhibited with 3% $H_2O_2$. The immunostained cells were imaged using an Olympus IX71 microscope (Olympus, Tokyo, Japan).

### Cytotoxicity Assay

Cell Counting Kit-8 (CCK-8) assay (Beyotime Biotechnology, Shanghai, China) followed by measuring the spectrophotometric absorbance at 450 nm was used to estimate cell proliferation. OFs were cultured at a density of $4 \times 10^3$ cells/well in 96-well plates in 0.1 mL DMEM supplemented with 10% FBS. All experiments were according to the manufacturer's instructions.

### RNA Isolation and Reverse Transcription

Cells were cultured in 6-cm plastic culture plates until they reached confluence. Cells for RNA isolation were harvested into TRIzol (TaKaRa Biotechnology, Dalian, China) reagent. Briefly, after the addition of 10% chloroform (Macklin Reagent, Beijing, China), cells were vortex mixed for 15 seconds and incubated for 10 minutes at room temperature. After centrifuging at 10000 × *g* for 10 minutes at 4°C, the top non-pink layer was transferred to a new microcentrifuge tube, and equal volume of isopropanol was added. The sample was incubated for 10 minutes at 4°C. After centrifuging the sample at 15000 × *g* for 10 minutes at 4°C, 1 mL 75% ethanol (prepared with diethyl pyrocarbonate water) was added, and washed the pellet by centrifugation at 10000 × *g* for 10 minutes at 4°C. Total RNA was eluted with 20 µL of sterile, RNase-free water. RNA quality was assessed for size and purity by using a NanoDrop 2000 Spectrophotometer (Thermo Scientific, Waltham, MA, USA). For reverse transcription of isolated RNA into cDNA, 1 µg of the extracted total RNA was subjected to reverse transcription using reverse-transcription kit (TaKaRa Biotechnology) according to the manufacturers' instructions, and the cDNA was stored at −80°C until use.

### Real-Time Quantitative PCR

The cDNA from the cells was used as the template for real-time quantitative PCR (RT-qPCR) amplification on an ABI 7500 Real-Time PCR system (Applied Biosystems, Foster City, CA, USA) using SYBR Premix Ex TaqII (TaKaRa Biotechnology). In separate experiments, RT-qPCR was performed to quantitatively assess the transcript levels of *IL-6*, *IL-8*, *TNF-α*, *CCL2*, *α-SMA*, *COL1A2*, *HAS2*, *FN1*, and *GAPDH* in cell samples using the gene-specific primers shown in Table 2. Initially, cDNA was denatured at 95°C for 30 seconds. Afterward, 40 PCR cycles (95°C 5 seconds and 60°C 34 seconds for each cycle) were run. Target gene expression levels were normalized to that of *GAPDH*, and the results are expressed as the fold change in cycle threshold (Ct) value relative to the control group as determined with the $2^{-\Delta\Delta Ct}$ method. Data were included in the analysis only if Ct value was <35.

### Enzyme-Linked Immunosorbent Assays (ELISA)

Cell-free supernatants were collected and centrifuged at 300 × *g* for 10 minutes at room temperature and stored at –80°C until analysis. The expression levels of IL-6, TNF-α, C-C motif chemokine ligand 2 (CCL2), alpha-smooth muscle actin (α-SMA), collagen type 1 (Col 1), hyaluronic acid (HA), and fibronectin (FN) in the culture supernatant of confluent OFs were determined using commercially available ELISA kits (IL-6, TNF-α, and CCL2 purchased from Multisciences, Hangzhou, China; α-SMA and FN purchased from Lianshuo Biological Technology, Shanghai, China; Col 1 and HA purchased from Enzyme-linked Biotechnology, Shanghai, China) according to the manufacturers' instructions. Each sample was tested three times. All samples were tested in the same assay.

**Table 2.** Primer Sequences of RT-qPCR

| Genes | Sequences (5′-3′) |
|---|---|
| *IL-6* | F: AAGCCAGAGCTGTGCAGATGAGTA |
| | R: TGTCCTGCAGCCACTGGTTC |
| *IL-8* | F: AACTGAGAGTGATTGAGAGTGG |
| | R: ATGAATTCTCAGCCCTCTTCAA |
| *TNF-α* | F: CTGCCTGCTGCACTTTGGAG |
| | R: ACATGGGCTACAGGCTTGTCACT |
| *CCL2* | F: CATAGCAGCCACCTTCATTCC |
| | R: TCTCCTTGGCCACAATGGTC |
| *α-SMA* | F: CTCTGGACGCACAACTGGCATC |
| | R: CACGCTCAGCAGTAGTAACGAAGG |
| *COL1A2* | F: CTGGACCTCCAGGTGTAAGC |
| | R: TGGCTGAGTCTCAAGTCACG |
| *HAS2* | F: CACGTAACGCAATTGGTCTTGTC |
| | R: CCAGTGCTCTGAAGGCTGTGTAC |
| *FN1* | F: ACAAGCATGTCTCTCTGCCA |
| | R: TTTGCATCTTGGTTGGCTGC |
| *GAPDH* | F: GACAGTCAGCCGCATCTTCT |
| | R: GCGCCCAATACGACCAAATC |

### Western Blotting Analysis

As primary antibodies, a rabbit anti-nuclear factor-κ B (NF-κB) (diluted 1:1000, Cell Signaling Technology, Danvers, MA, USA), a rabbit anti-TLR4 (diluted 1:1000, Cell Signaling Technology), a rabbit anti-SMAD2 (diluted 1:1000, Cell Signaling Technology), a rabbit anti-p-SMAD2 (diluted 1:1000, Cell Signaling Technology), a rabbit anti-SMAD3 (diluted 1:1000, Sangon Biotech), a rabbit anti-p-SMAD3 (diluted 1:1000, Sangon Biotech), and a rabbit anti-SMAD4 (diluted 1:1000, Wanleibio, Shenyang, China) were used. Protein extracts were stored at –80°C until use. Equal amounts of denatured protein were subjected to 10% sodium dodecyl sulfate polyacrylamide gel electrophoresis, and the separated proteins were transferred to polyvinylidene difluoride membranes (Solarbio Life Sciences, Beijing, China). Nonspecific binding was blocked with BSA (Dalian Meilun Biotechnology) for 1 hour at room temperature. The membranes were then incubated overnight at 4°C with antibodies against NF-κB, SMAD2, p-SMAD2, SMAD3, p-SMAD3, SMAD4, and β-actin at the dilutions specified by the manufacturers. The membranes were then incubated with anti-rabbit IgG (DyLight 680 Conjugate; Cell Signaling Technology) forx 2 hours at room temperature. The protein bands were imaged with a LI-COR automatic chemiluminescence image analysis system (LI-COR, Nebraska USA). Quantification of Western blotting signals was achieved with Odyssey Fc Imaging System (LI-COR, Nebraska USA).

### Statistics

Statistical analyses were performed using GraphPad Prism (v8.2.0 for macOS) software (GraphPad Software, San Diego,

Investigative Ophthalmology & Visual Science

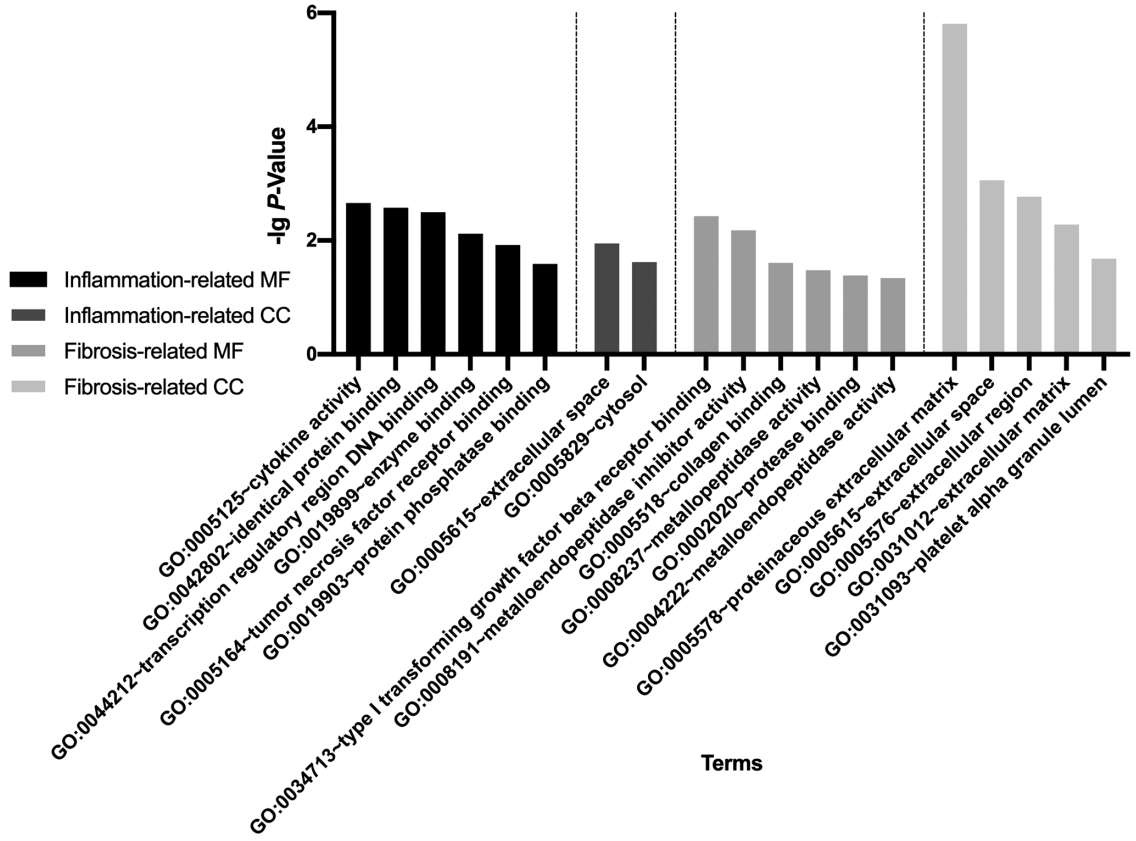


**Figure 1.** Gene ontology analysis results. The inflammation-related gene targets were mainly associated with cytokine activity, TNF receptor binding, extracellular space, and cytosol. The fibrosis-related targets were principally involving type 1 TGF-$\beta$ receptor binding, collagen binding, proteinaceous extracellular matrix, and extracellular space. MF, molecular function; CC, cellular component.

CA, USA). Significance tests of different culture conditions were conducted using 1-way ANOVA, and 2-way ANOVA was used to examine the significance between GO and non-GO in different culture conditions. Bar charts were generated using means and the standard deviation (SD). $P$ values less than 0.05 were considered as statistically significant ($^{*}P < 0.05$, $^{**}P < 0.01$, $^{***}P < 0.001$, $^{****}P < 0.0001$).

## Results

### Bioinformatics Analysis

Based on the literature screening,[18,22–34] eight inflammatory cytokine-encoding genes and nine fibrotic mediator-encoding genes were identified as being related to Gyps' function. Inflammation-related targets were TNF, IL-1$\beta$, IL-5, mitogen-activated protein kinase 14, NF-$\kappa$B subunit 1, signal transducer and activator of transcription 1, peroxisome proliferator activated receptor gamma and vascular cell adhesion molecule 1, and fibrosis-related targets were matrix metallopeptidase 2, matrix metallopeptidase 9, TIMP metallopeptidase inhibitor 1, TIMP metallopeptidase inhibitor 2, TGF-$\beta$1, SMAD family member 7, cellular communication network factor 2, aldehyde dehydrogenase 1 family member B1, and peroxisome proliferator activated receptor $\alpha$.

The significantly enriched (cut-of criterion with statistic difference was $P < 0.05$) gene ontology categories are shown in Figure 1. Through molecular functions and cellular components analyses, the inflammation-related genes were mainly associated with cytokine activity (GO:0005125), TNF receptor binding (GO:0005164), extracellular space (GO:0005615), and cytosol (GO:0005829). The fibrosis-related genes were principally involved in type 1 TGF-$\beta$ receptor binding (GO:0034713), collagen binding (GO:0005518), proteinaceous extracellular matrix (GO:0005578), and extracellular space (GO:0005615). The results for biological processes–related gene ontologies are shown in Supplementary Tables S1 and S2.

The most significant Reactome pathways of the selected genes were mainly enriched in IL-1 processing (R-HSA-448706), activation of matrix metalloproteinases (R-HSA-1592389), downregulation of TGF-$\beta$ receptor signaling (R-HSA-2173788), and collagen degradation (R-HSA-1442490) (Fig. 2). The KEGG analysis a re shown in Supplementary Tables S3 and S4.

### Cell Identification

Primary cells were cultured from GO and non-GO patient-derived retrobulbar orbital connective tissues. VIM is present in cells of mesoderm origin, such as fibroblasts. The positive expression of VIM observed in our study demonstrated that the cells were fibroblasts (Fig. 3A). Additionally, the negative expressions of DES, KRT17, MB, S100B excluded smooth muscle cells and cardiomyocytes, skin cells, muscle and striated muscle, nerve cells and skin melanocytes, respectively (Figs. 3B–E), with negative control slides shown in Figures 3F–J. Consequently, the cells we obtained from orbit were identified as OFs. Bright field image (magnification $\times$

Investigative Ophthalmology & Visual Science

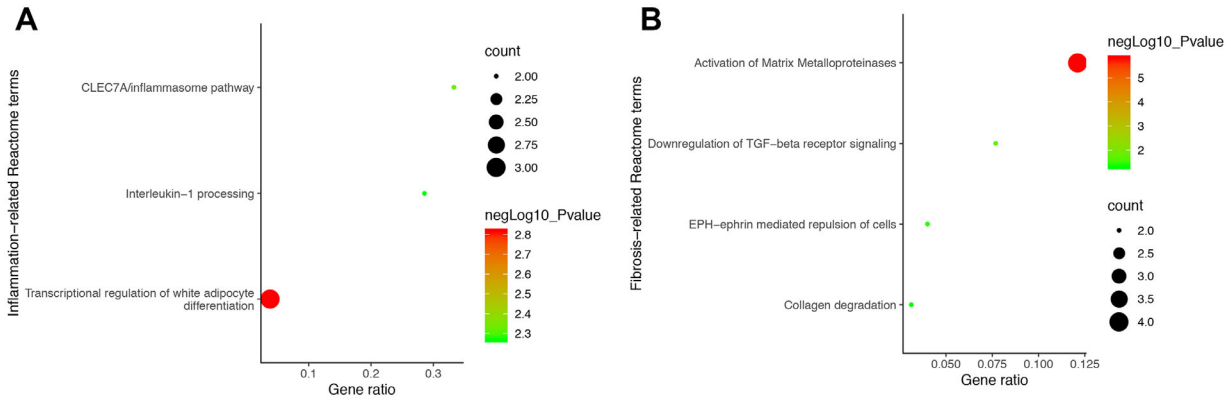


**Figure 2.** Reactome pathway analysis results. The inflammation-related gene targets were mainly enriched at transcriptional regulation of white adipocyte differentiation, CLEC7A/inflammasome pathway, and IL-1 processing (**A**). The fibrosis-related targets were mainly enriched at activation of matrix metalloproteinases, downregulation of TGF-$\beta$ receptor signaling, EPH-ephrin mediated repulsion of cells, and collagen degradation (**B**).

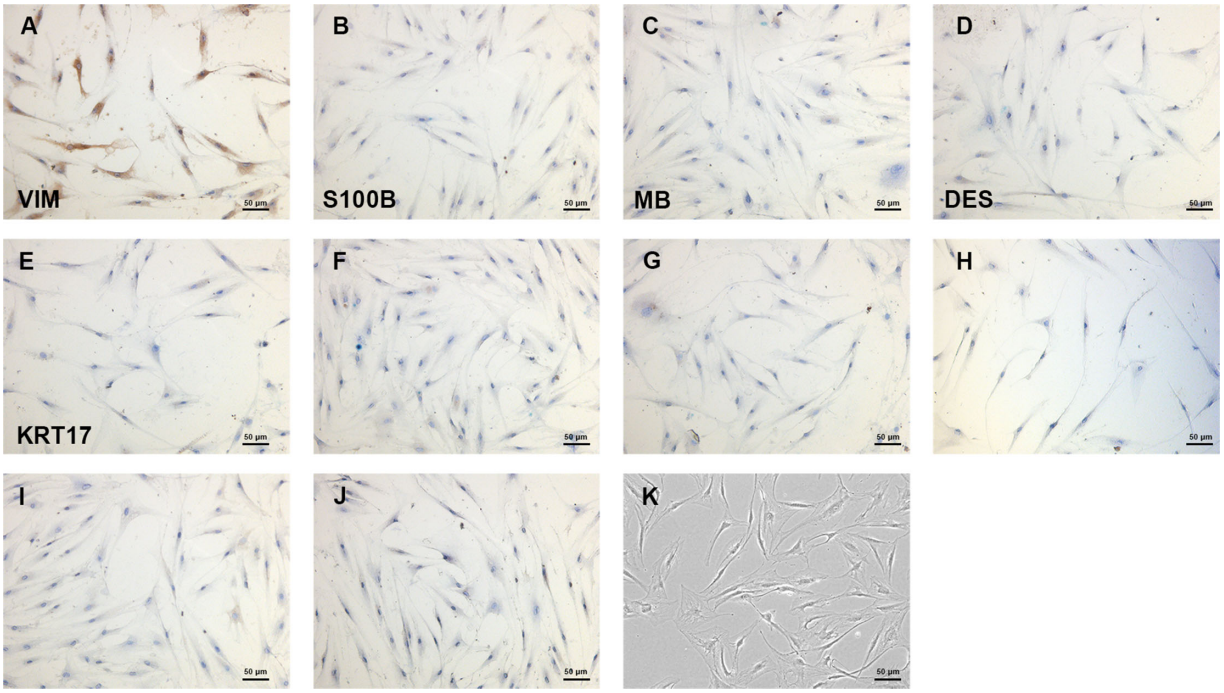


**Figure 3.** Immunohistology analysis showed positive expression of VIM (**A**), negative expression of S100B (**B**), MB (**C**), DES (**D**), and KRT17 (**E**), and corresponding negative controls (**F–J**). Cell morphology was shown in bright field images (magnification × 100, **K**), the identity of OFs was verified by immunohistology analysis.

100) is shown in Figure 3K. Cells with negative VIM expression were considered as non-OFs.

## Gyps Promote OF Proliferation

The effect of Gyps on the proliferation of OFs was investigated by CCK-8 assay in vitro. OFs were treated with Gyps at indicated concentrations for 24 and 48 hours (Fig. 4). The results showed that Gyps significantly enhanced OF proliferation at 24 hours at 25, 50, 100, 250, 500, and 1000 μg/mL, with 100 μg/mL having the most obvious effect (1-way ANOVA, $P < 0.01$). However, this effect did not persist over 48 hours (Fig. 4). Additionally, no significant differences were observed between GO and non-GO at the same concentration of Gyps at both 24 and 48 hours (2-way ANOVA, all $P > 0.05$).

## Gyps Inhibit IL-1$\beta$-Induced Inflammation in OFs

RT-qPCR and ELISA assays were performed to investigate the effect of Gyps on IL-1$\beta$-induced inflammation. IL-1$\beta$ (10 ng/mL, 24 hours) elicited a marked (~2.5- to 40-fold) and significant increase in the mRNA levels of *IL-6*, *IL-8*, *TNF-α*, and *CCL2* in ex vivo–cultured primary OFs (Fig. 5). In addition to mRNA expressions, the protein levels of IL-6, CCL2, and TNF-$\alpha$ in cell culture supernatant were also increased significantly (Fig. 6). Pretreating OFs with Gyps (100 μg/mL, 24 hours), however, prevented IL-1$\beta$-induced

Investigative Ophthalmology & Visual Science

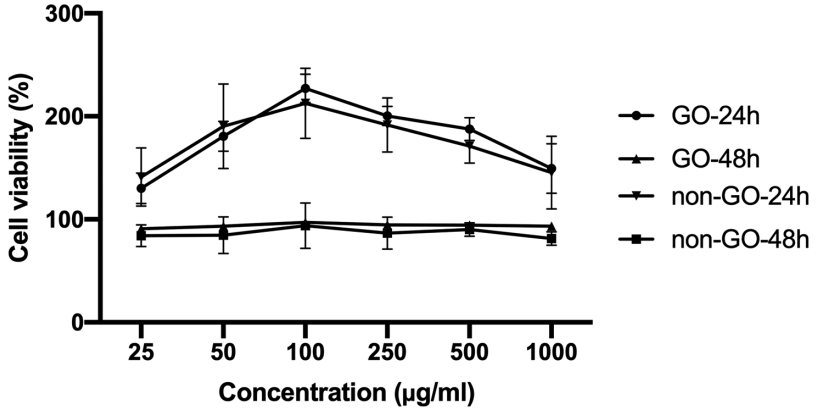


**Figure 4.** Cytotoxicity study using CCK-8 assay. GO (n = 6) and non-GO (n = 4) OFs were treated with Gyps at desired concentrations for 24 and 48 hours. The cell proliferation was significantly increased under the stimulation of 100 μg/mL Gyps, and this effect did not persist over 48 hours.

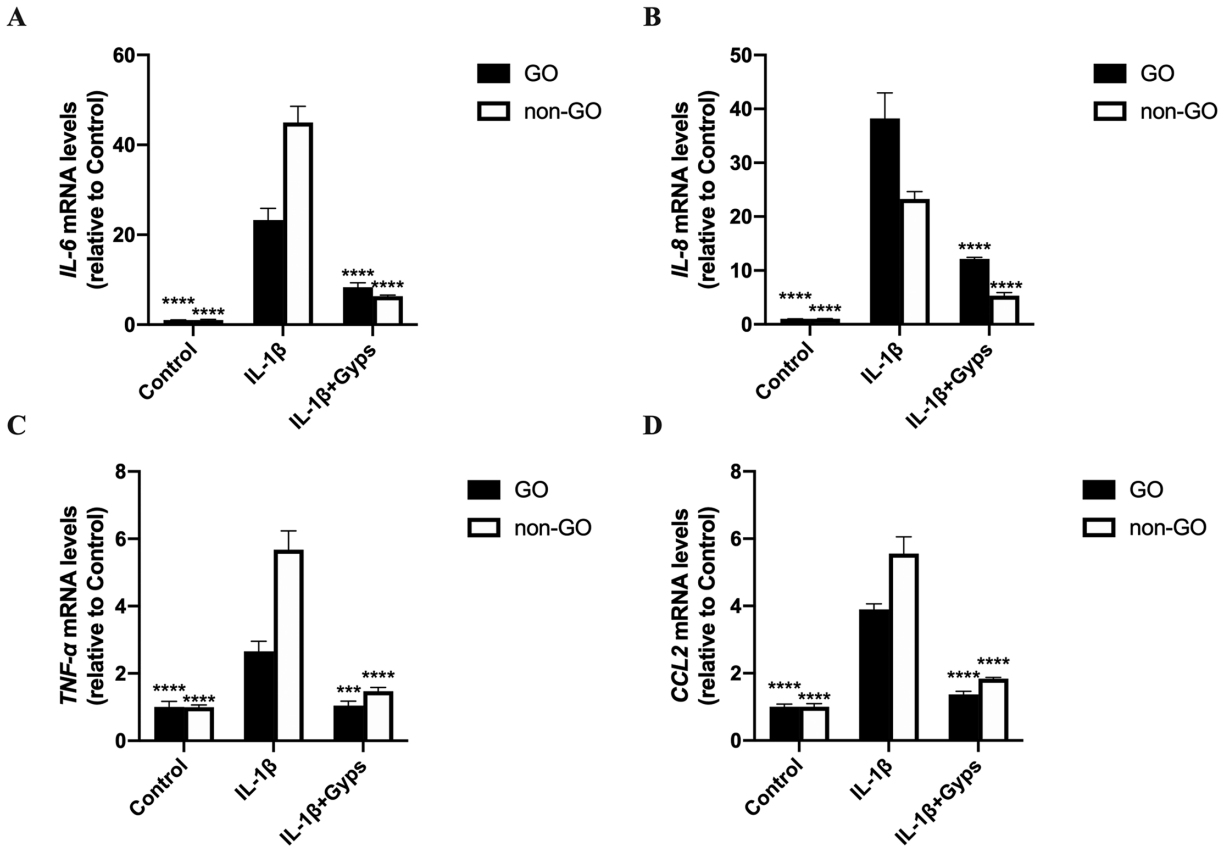


**Figure 5.** The mRNA levels of inflammation-related cytokines (*IL-6*, *IL-8*, *TNF-α*, and *CCL2*) in OFs. Go (n = 6) and non-GO (n = 4) OFs were treated with 10 ng/mL IL-1$\beta$ for 24 hours in the absence or presence of pretreating with 100 μg/mL Gyps for 24 hours. The expression of *IL-6* (**A**), *IL-8* (**B**), *TNF-α* (**C**), and *CCL2* (**D**) mRNA in each cell group was evaluated by RT-qPCR. ***$P < 0.001$ and ****$P < 0.0001$ versus IL-1$\beta$-stimulated cells, 1-way ANOVA.

increase in *IL-6*, *IL-8*, *TNF-α*, and *CCL2* mRNA expression (Fig. 5), as well as the increased protein secretion of IL-6, TNF-α, and CCL2 (Fig. 6). For mRNA levels, *IL-6*, *TNF-α*, and *CCL2*, mRNA expressed significantly higher in non-GO IL-1$\beta$-treated groups (2-way ANOVA, all $P < 0.0001$). The protein levels of IL-6, CCL2, and TNF-α in GO IL-1$\beta$-treated groups were significantly higher than non-GO groups (2-way ANOVA, all $P < 0.001$). In addition, the protein level of IL-6 and CCL2 in GO Gyps-treated groups were higher (2-way ANOVA, all $P < 0.0001$).

## Gyps Inhibit TGF-$\beta$1-Induced Fibrosis in OFs

RT-qPCR and ELISA assays were performed to investigate the effect of Gyps on TGF-$\beta$1-induced fibrosis. Stimulation of OFs with TGF-$\beta$1 (10 ng/mL, 24 hours) elicited a marked

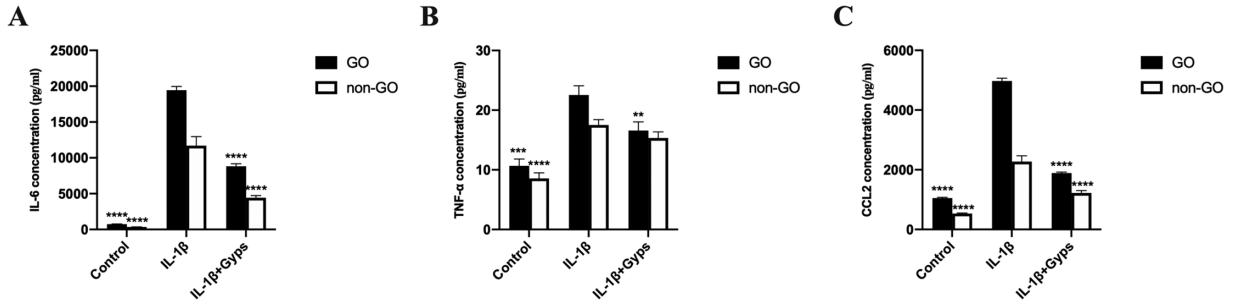


**Figure 6.** The protein levels of inflammation-related cytokines in OF culture supernatant. Go (n = 6) and non-GO (n = 4) OFs were treated with 10 ng/mL IL-1$\beta$ for 24 hours in the absence or presence of pretreating with 100 µg/mL Gyps for 24 hours. The production of IL-6 (**A**), TNF-$\alpha$ (**B**), and CCL2 (**C**) in each cell group was evaluated by ELISA assay. $^{**}P < 0.01$, $^{***}P < 0.001$, and $^{****}P < 0.0001$ versus IL-1$\beta$-stimulated cells, 1-way ANOVA.

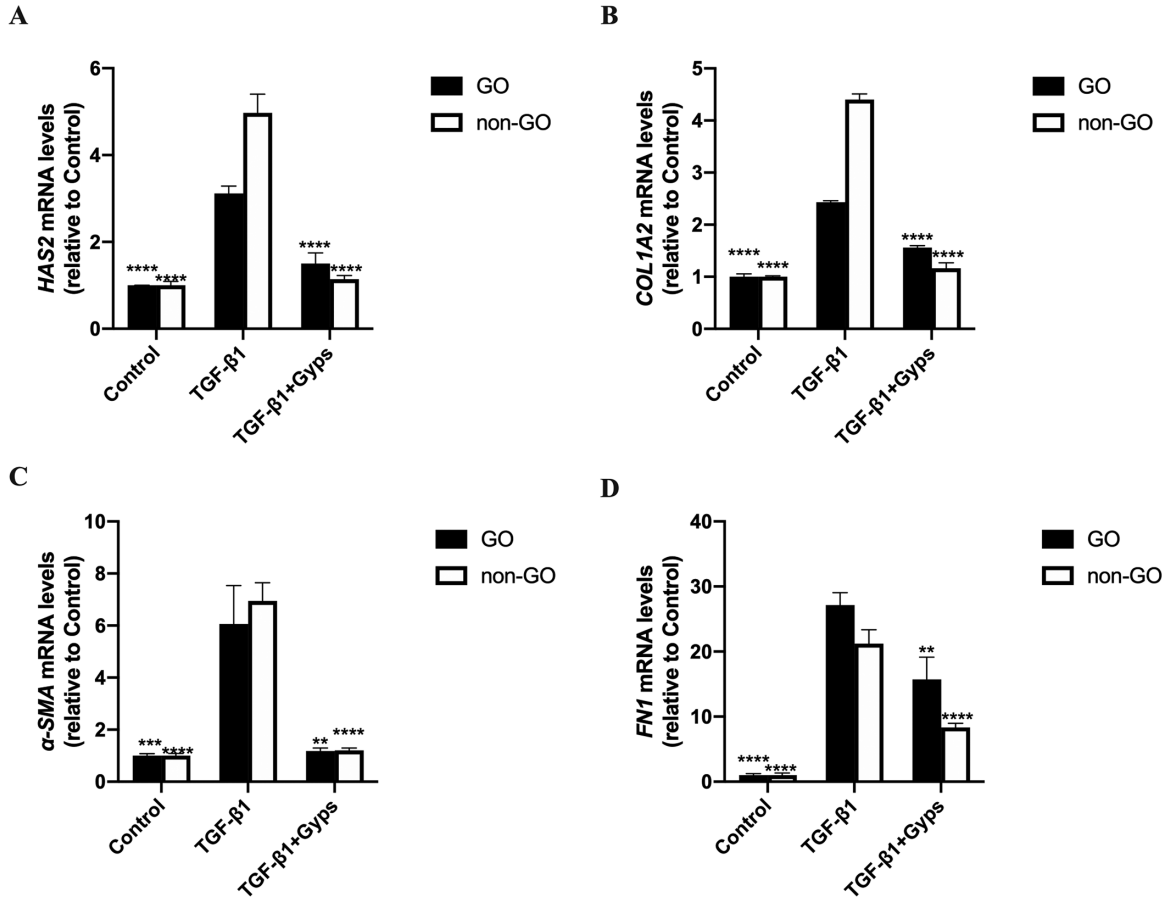


**Figure 7.** The mRNA levels of fibrotic mediators in OFs. Go (n = 6) and non-GO (n = 4) OFs were treated with 10 ng/mL TGF-$\beta$1 for 24 hours in the absence or presence of pretreating with 100 µg/mL Gyps for 24 hours. The expression of *HAS2* (**A**), *COL1A2* (**B**), *α-SMA* (**C**), and *FN1* (**D**) mRNA in each cell group was evaluated by RT-qPCR. $^{**}P < 0.01$, $^{***}P < 0.001$, and $^{****}P < 0.0001$ versus TGF-$\beta$1-stimulated cells, 1-way ANOVA.

(~2.5- to 25-fold) and significant increase in the mRNA expression of *HAS2*, *COL1A2*, *α-SMA*, and *FN1* (Fig. 7). Similarly, the protein levels of HA, Col 1, α-SMA, and FN expression in cell culture supernatant were increased significantly as well (Fig. 8). Pretreatment with Gyps (100 µg/mL, 24 hours) prevented TGF-$\beta$1-induced increases of *HAS2*, *COL1A2*, *α-SMA*, and *FN1* mRNA expression (Fig. 7), and HA, Col 1, α-SMA, and FN (Fig. 8) protein levels in OF culture media. The mRNA levels of *HAS2* and *COL1A2* were significantly higher in non-GO TGF-$\beta$1-treated group (2-way ANOVA, all $P < 0.0001$), in contrast to *FN1* (2-way ANOVA, $P < 0.01$). However, no difference was observed between *α-SMA* of GO and non-GO in TGF-$\beta$1-treated group (2-way ANOVA, $P > 0.05$). The mRNA levels of *COL1A2* and *FN1* in GO Gyps-treated groups were higher than that in non-GO (2-way ANOVA, all $P < 0.01$). The protein levels of HA, Col 1, α-SMA, and FN in GO TGF-$\beta$1-treated groups were significantly higher than non-GO groups (2-way ANOVA, all

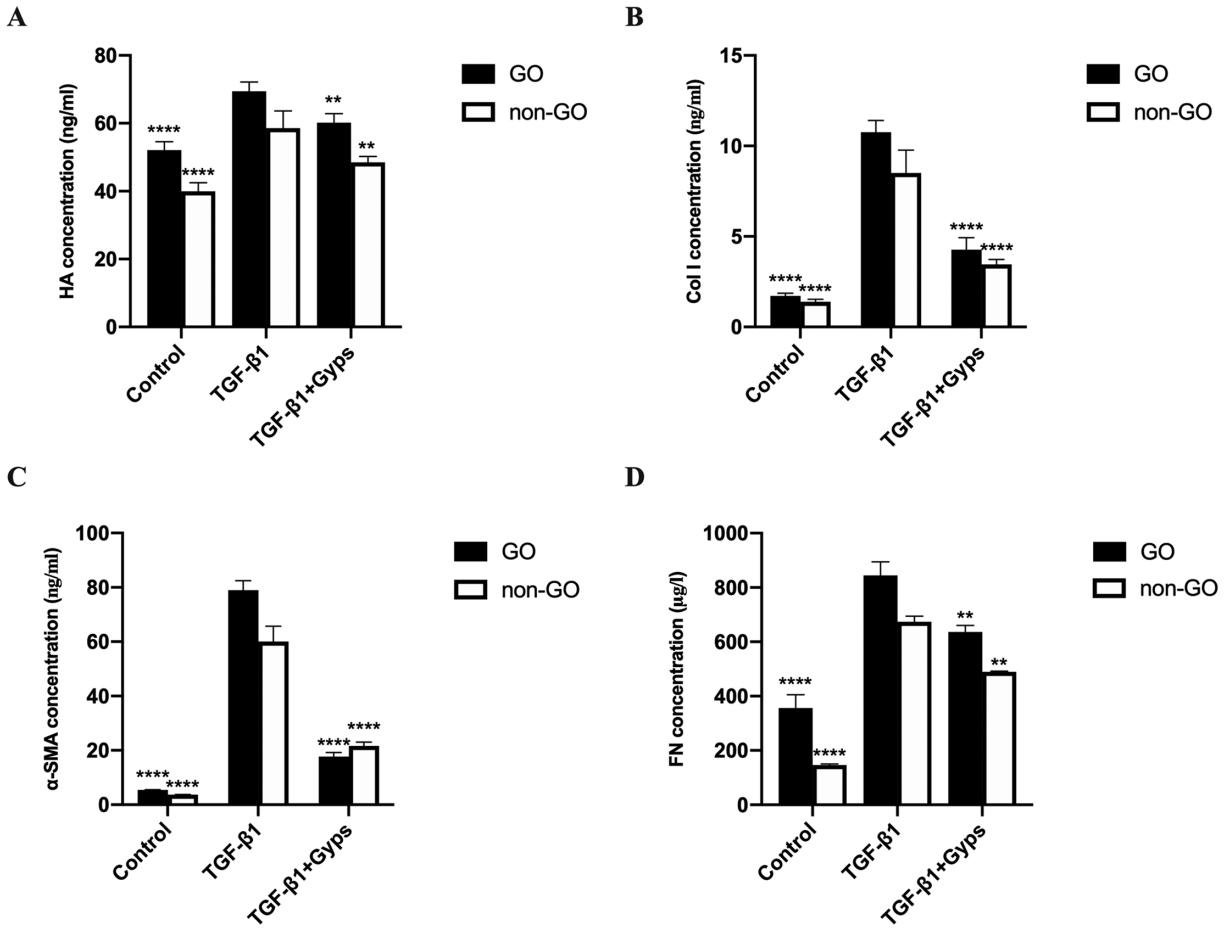


**Figure 8.** The protein levels of fibrotic mediators in OF culture supernatant. Go (n = 6) and non-GO (n = 4) OFs were treated with 10 ng/mL IL-1$\beta$ for 24 hours in the absence or presence of pretreating with 100 μg/mL Gyps for 24 hours. The production of HA (**A**), Col 1 (**B**), $\alpha$-SMA (**C**), and FN (**D**) protein in each cell group was evaluated by ELISA assay. $^{**}P < 0.01$ and $^{****}P < 0.0001$ versus TGF-$\beta$1-stimulated cells, 1-way ANOVA.

$P < 0.01$). Additionally, the protein levels of HA and FN in GO Gyps-treated groups were higher (2-way ANOVA, all $P < 0.001$).

### Gyps Anti-Inflammatory Effect is Mediated Through TLR4/NF-$\kappa$B Signaling

To clarify the role of Gyps in TLR4/NF-$\kappa$B signaling, Western blotting assay was conducted. Consistent with the observed increases in inflammation-related mRNA expression, TLR4 and NF-$\kappa$B were significantly increased in IL-1$\beta$ (10 ng/mL, 24 hours) group (Fig. 9A for GO and Fig. 10A for non-GO). Gyps (100 μg/mL, 24 hours) treatment obviously decreased the IL-1$\beta$-induced activation of TLR4/NF-$\kappa$B signaling pathway (Fig. 9A for GO and Fig. 10A for non-GO).

### Gyps Anti-Fibrosis Effect is Mediated Through SMADs Signaling

Previous research indicated that the TGF-$\beta$1-induced $\alpha$-SMA upregulation was mainly mediated by SMAD signaling pathway. To quantify the expression and activation of SMAD2/4 in OFs, Western blotting assay was conducted. Consistent with our previous findings that fibrosis-related mRNAs were increased by TGF-$\beta$1 (10 ng/mL) treatment, the levels of SMAD2, p-SMAD2, and SMAD4 were significantly increased in OFs challenged with TGF-$\beta$1 (Figs. 9B–D for GO and Figs. 10B–D for non-GO). Gyps (100 μg/mL, 24 hours) treatment obviously decreased the TGF-$\beta$1-induced activation of SMAD2/4 signaling pathway (Figs. 9B–D for GO and Figs. 10B–D for non-GO).

## Discussion

GO seriously affects the appearance and visual function of patients. It has been shown that the functions of OFs are regulated not only by inflammatory factors secreted by T cells, B cells, macrophages, and mast cells, but also by surface receptors, such as TSHR and IGF-1R. These cytokines and receptors mediate the pathological processes of GO by modulating cell proliferation, inflammatory factor secretion, extracellular matrix synthesis, and fibrosis.[8] The immune inflammatory reaction, fibrosis, and oxidation of OFs are important factors for the occurrence and development of GO and are important targets in GO treatment. At present, there are still many limitations in the treatment of GO, finding new drugs with better therapeutic effects and fewer side effects are particularly urgent for the treatment of orbital

Investigative Ophthalmology & Visual Science

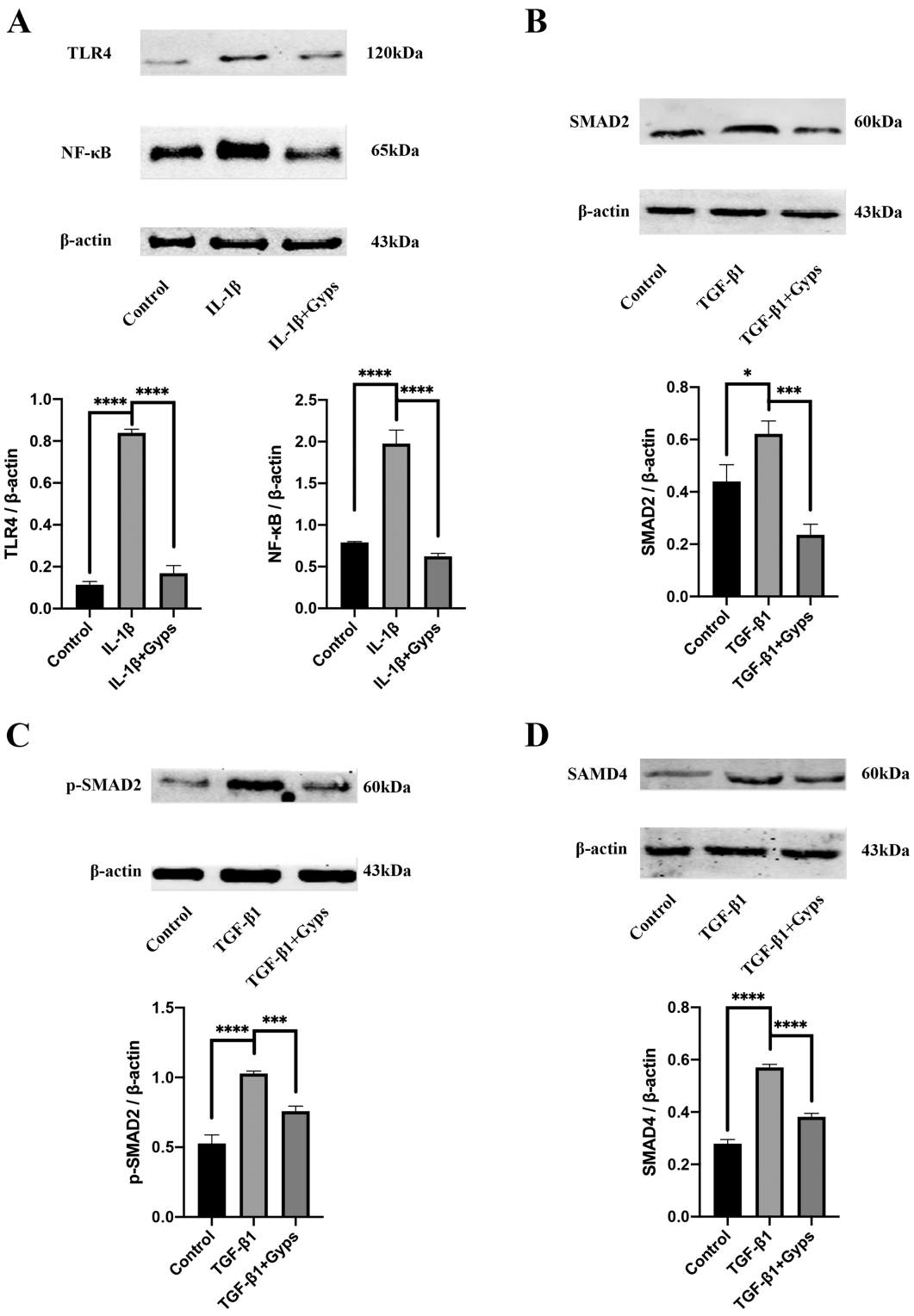


**Figure 9.** Effects of Gyps on inflammation- and fibrosis-related signaling pathways in GO OFs. Expression levels of TLR4 (**A**) and NF-$\kappa$B (**A**) in GO (n = 6) OFs were evaluated after treatment with IL-1$\beta$ (10 ng/mL, 24 hours) in the absence or presence of pretreating with Gyps (100 µg/mL, 24 hours). Expression levels of SMAD2 (**B**), p-SMAD2 (**C**), and SMAD4 (**D**) in GO (n = 6) OFs were evaluated after treatment with TGF-$\beta$1 (10 ng/mL, 24 hours) in the absence or presence of pretreating with Gyps (100 µg/mL, 24 hours). *$P < 0.05$, ***$P < 0.001$, and ****$P < 0.0001$, 1-way ANOVA.

inflammation and fibrosis. In this study, we found that IL-1$\beta$ stimulated OFs to produce inflammatory factors, such as IL-6, IL-8, TNF-$\alpha$, and MCP-1, via regulating NF-$\kappa$B signaling pathway. Although TGF-$\beta$1 promoted the secretion of $\alpha$-SMA, FN, HA, and Col 1 via regulating SMAD signaling pathway. In addition, Gyps prevented inflammation and fibrosis-

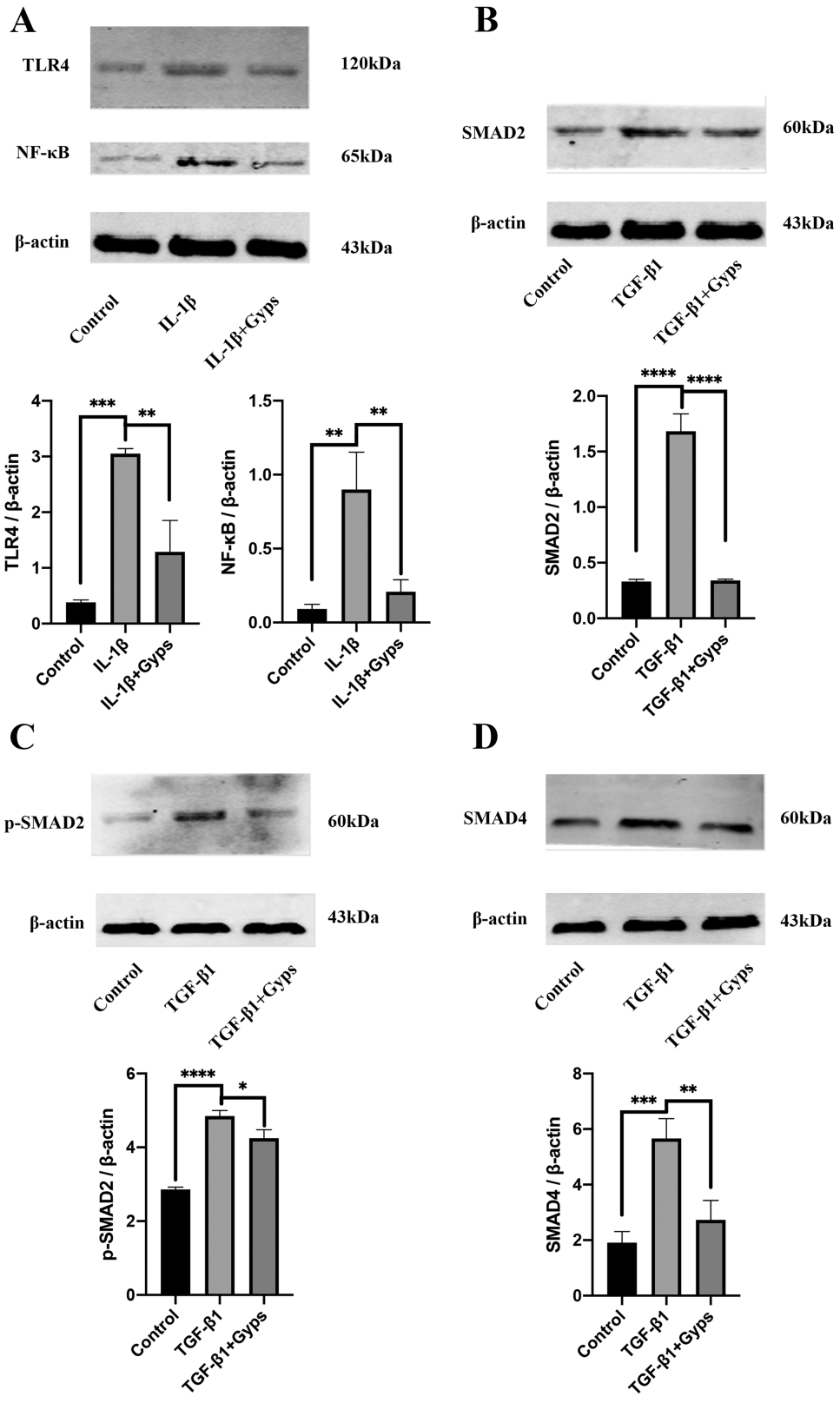


**Figure 10.** Effects of Gyps on inflammation- and fibrosis-related signaling pathways in non-GO OFs. Expression levels of TLR4 (**A**) and NF-$\kappa$B (**A**) in non-GO (n = 4) OFs were evaluated after treatment with IL-1$\beta$ (10 ng/mL, 24 hours) in the absence or presence of pretreating with Gyps (100 µg/mL, 24 hours). Expression levels of SMAD2 (**B**), p-SMAD2 (**C**), and SMAD4 (**D**) in non-GO (n = 4) OFs were evaluated after treatment with TGF-$\beta$1 (10 ng/mL, 24 hours) in the absence or presence of pretreating with Gyps (100 µg/mL, 24 hours). *$P < 0.05$, **$P < 0.01$, ***$P < 0.001$, and ****$P < 0.0001$, 1-way ANOVA.

related changes induced by IL-1$\beta$ and TGF-$\beta$1 in OFs, and then reduced the apoptosis of OFs. Moreover, we found that Gyps displayed its biological effects on OFs even at a low concentration. The discrepancies between GO and non-GO OFs in control, stimulated, and Gyps-treated groups were not completely consistent, however, most of the indicators' mRNA expression and protein secretion levels were statistically lower in non-GO group after treatment of Gyps. Potential underlying mechanism remains to be determined. This study is helpful to explain the action mechanisms of Gyps in the treatment of orbital inflammation and fibrosis in GO.

It has been extensively characterized that IL-1$\beta$ played a primary role in a variety of cell activities, including immune response and cell apoptosis.[35] Furthermore, inflammation plays a dominant role in the early histopathology of GO. IL-1$\beta$ is a member of the IL-1 cytokine family and serves as an important mediator of inflammation.[36] It has been found that IL-1$\beta$ increased the autophagy activity of GO cells, and inhibited the adipogenic differentiation of preadipocytes by blocking autophagy induced by bafilomycin A1 treatment or ATG-5 knockout, which is reported to contribute to GO pathogenesis.[37] In this study, IL-1$\beta$ was used to establish the inflammatory model of OFs to further study the anti-inflammatory effect of Gyps. Additionally, orbital fibrosis is mediated by a variety of inflammatory factors and mechanical stimulation, including TGF-$\beta$ family (TGF-$\beta$1, TGF-$\beta$2, and TGF-$\beta$3). TGF-$\beta$s are regarded as an essential factor associated with many eye tissue fibrosis, including corneal opacification, pterygium, proliferative vitreoretinopathy, and conjunctival fibrosis after glaucoma surgery.[38] Among them, TGF-$\beta$1 has been shown to stimulate myofibroblasts differentiation, extracellular matrix synthesis or fibroblasts of corneal fibroblasts, conjunctival fibroblasts, and OFs.[39–42] Thus TGF-$\beta$1 was used to establish the fibrosis model of OFs to study the anti-fibrosis effect of Gyps. Because of the shorter effects of IL-1$\beta$/TGF-$\beta$1 in vitro, IL-1$\beta$ and TGF-$\beta$1 were given after Gyps treatment to achieve the best drug stimulation effect and determine the effect of Gyps. NF-$\kappa$B is a central transcription factor activated by many inflammatory cytokines, including IL-1$\beta$, and widely participates in the regulation of immune responses and inflammation.[43] SMADs are crucial transcription factors in TGF-$\beta$1 signaling and participate in animal embryonic development and tissue regeneration.[44] Previous reports have shown that the differentiation of myofibroblasts was regulated by TGF-$\beta$/SMAD signaling pathway.[45,46] Hence NF-$\kappa$B and SMAD pathways are important signaling pathways related to GO-related inflammation and fibrosis, respectively.

Gyps are the main components in the extract of *Gynostemma pentaphyllum*. They are popular Chinese herbal extracts in China, serving as characteristic drugs of the Zhuang nationality in Guangxi Province.[47] Studies have previously shown that Gyps were widely used because of its anti-inflammatory, anti-tumor, immune enhancement, anti-ulcer, antioxidant, and anti-aging effects.[48–50] In this present study, we first studied the anti-inflammatory and anti-fibrosis functions of Gyps in GO-related inflammation and fibrosis in vitro. We found that the expression and secretion of inflammatory cytokines (IL-6, IL-8, TNF-$\alpha$, and MCP-1) were increased after IL-1$\beta$ stimulation. Additionally, the expression and secretion of fibrotic factors (HA, $\alpha$-SMA, FN, and Col-1, and extracellular matrix[51]) were increased after TGF-$\beta$1 stimulation in OFs. Although all of these mediators were decreased after treatment with Gyps. Besides, Gyps could also inhibit NF-$\kappa$B signaling pathway and SMAD signaling pathway in OFs. These data suggested that Gyps can not only reduce orbital inflammation, but also inhibit the fibrosis in OFs.

## Conclusions

Although Gyps could be considered as a complementary treatment for GO, however, this study only investigated the ex vivo effects of Gyps on ex vivo cultured OFs, further studies and clinical trials are needed to verify its effects on GO patients. In summary, our study identified the roles of Gyps in suppressing the inflammation and fibrosis of OFs from GO patients by inhibiting NF-$\kappa$B and SMAD signaling pathways. These findings suggest that Gyps are promising complementary anti-inflammatory and anti-fibrosis drugs for GO.

### *Acknowledgments*

The authors thank 51runse, Toweree (Beijing) Education Company, for editing the manuscript.

Supported by the National Natural Science Foundation of China (No. 81360152); the Guangxi Natural Science Foundation (No. 2018GXNSFAA281234); 2019 Guangxi One Thousand Young and Middle-Aged College and University Backbone Teachers Cultivation Program; and "Medical Excellence Award" funded by the Creative Research Development grant from the First Affiliated Hospital of Guangxi Medical University.

Disclosure: **H. Li,** None; **C. Ma**, None; **W. Liu**, None; **J. He**, None; and **K. Li,** None

### *References*

1. Perros P, Krassas GE. Graves orbitopathy: a perspective. *Nat Rev Endocrinol*. 2009;5:312–318.
2. Pappa A, Lawson JM, Calder V, Fells P, Lightman S. T cells and fibroblasts in affected extraocular muscles in early and late thyroid associated ophthalmopathy. *Br J Ophthalmol*. 2000;84:517–522.
3. Menconi F, Profilo MA, Leo M, et al. Spontaneous improvement of untreated mild Graves' ophthalmopathy: Rundle's curve revisited. *Thyroid*. 2014;24:60–66.
4. Eckstein AK. Thyroid associated ophthalmopathy: evidence for CD4+T cells; de novo differentiation of RFD7+ macrophages, but not of RFD1+ dendritic cells; and loss of and T cell receptor expression. *Br J Ophthalmol*. 2004;88:803–808.
5. Sahli E, Gunduz K. Thyroid-associated ophthalmopathy. *Turk J Ophthalmol*. 2017;47:94–105.
6. van Steensel L, Paridaens D, van Meurs M, et al. Orbit-infiltrating mast cells, monocytes, and macrophages produce PDGF isoforms that orchestrate orbital fibroblast activation in Graves' ophthalmopathy. *J Clin Endocrinol Metab*. 2012;97:E400–E408.
7. Bahn RS. Graves' ophthalmopathy. *N Engl J Med*. 2010;362:726–738.
8. Dik WA, Virakul S, van Steensel L. Current perspectives on the role of orbital fibroblasts in the pathogenesis of Graves' ophthalmopathy. *Exp Eye Res*. 2016;142:83–91.
9. Chen B, Tsui S, Smith TJ. IL-1 induces IL-6 expression in human orbital fibroblasts: identification of an anatomic-site specific phenotypic attribute relevant to thyroid-associated ophthalmopathy. *J Immunol*. 2005;175:1310–1319.
10. Hwang CJ, Afifiyan N, Sand D, et al. Orbital fibroblasts from patients with thyroid-associated ophthalmopathy

overexpress CD40: CD154 hyperinduces IL-6, IL-8, and MCP-1. *Invest Ophthalmol Vis Sci*. 2009;50:2262–2268.

11. Shimizu T. Inflammation-inducing factors of *Mycoplasma pneumoniae*. *Front Microbiol*. 2016;7:414.
12. Smith TJ. TSH-receptor-expressing fibrocytes and thyroid-associated ophthalmopathy. *Nat Rev Endocrinol*. 2015;11:171–181.
13. Huang LS, Jiang P, Feghali-Bostwick C, et al. Lysocardiolipin acyltransferase regulates TGF-beta mediated lung fibroblast differentiation. *Free Radic Biol Med*. 2017;112:162–173.
14. Higashi AY, Aronow BJ, Dressler GR. Expression profiling of fibroblasts in chronic and acute disease models reveals novel pathways in kidney fibrosis. *J Am Soc Nephrol*. 2019;30:80–94.
15. Im SA, Choi HS, Hwang BY, Lee MK, Lee CK Augmentation of immune responses by oral administration of *Gynostemma pentaphyllum* ethanol extract. *Korean J Pharmacogn*. 2009;40:35–40.
16. Wan ZH, Zhao Q. Gypenoside inhibits interleukin-1beta-induced inflammatory response in human osteoarthritis chondrocytes. *J Biochem Mol Toxicol*. 2017;31:e21926.
17. Wong WY, Lee ML, Chan BD, et al. *Gynostemma pentaphyllumsaponins* attenuate inflammation in vitro and in vivo by inhibition of NF-$\kappa$B and STAT3 signaling. *Oncotarget*. 2017;8:87401–87414.
18. Chen J, Li X, Hu Y, et al. Gypenosides ameliorate carbon tetrachloride-induced liver fibrosis by inhibiting the differentiation of hepatic progenitor cells into myofibroblasts. *Am J Chin Med*. 2017;45:1061–1074.
19. Song YN, Dong S, Wei B, et al. Metabolomic mechanisms of gypenoside against liver fibrosis in rats: an integrative analysis of proteomics and metabolomics data. *PLoS One*. 2017;12:e0173598.
20. Huang da W, Sherman BT, Lempicki RA. Systematic and integrative analysis of large gene lists using DAVID bioinformatics resources. *Nat Protoc*. 2009;4:44–57.
21. Huang da W, Sherman BT, Lempicki RA. Bioinformatics enrichment tools: paths toward the comprehensive functional analysis of large gene lists. *Nucleic Acids Res*. 2009;37:1–13.
22. Aktan F, Henness S, Roufogalis BD, Ammit AJ. Gypenosides derived from *Gynostemma pentaphyllum* suppress NO synthesis in murine macrophages by inhibiting iNOS enzymatic activity and attenuating NF-kappaB-mediated iNOS protein expression. *Nitric Oxide*. 2003;8:235–242.
23. Bae UJ, Park EO, Park J, et al. Gypenoside UL4-rich *Gynostemma pentaphyllum* extract exerts a hepatoprotective effect on diet-induced nonalcoholic fatty liver disease. *Am J Chin Med*. 2018;46:1315–1332.
24. Chen J, Zhang X, Xu Y, et al. Hepatic progenitor cells contribute to the progression of 2-acetylaminofluorene/carbon tetrachloride-induced cirrhosis via the non-canonical Wnt pathway. *PLoS One*. 2015;10:e0130310.
25. Chen JC, Tsai CC, Chen LD, Chen HH, Wang WC. Therapeutic effect of gypenoside on chronic liver injury and fibrosis induced by CCl4 in rats. *Am J Chin Med*. 2000;28:175–185.
26. Feng Q, Li X, Peng J, et al. Effect of gypenosides on DMN-induced liver fibrosis in rats. *Zhongguo Zhong Yao Za Zhi*. 2012;37:505–508.
27. Friedman SL. Mechanisms of hepatic fibrogenesis. *Gastroenterology*. 2008;134:1655–1669.
28. Gauhar R, Hwang SL, Jeong SS, et al. Heat-processed *Gynostemma pentaphyllum* extract improves obesity in ob/ob mice by activating AMP-activated protein kinase. *Biotechnol Lett*. 2012;34:1607–1616.
29. Gou SH, Huang HF, Chen XY, et al. Lipid-lowering, hepatoprotective, and atheroprotective effects of the mixture Hong-Qu and gypenosides in hyperlipidemia with NAFLD rats. *J Chin Med Assoc*. 2016;79:111–121.
30. Gou SH, Liu BJ, Han XF, et al. Anti-atherosclerotic effect of Fermentum Rubrum and *Gynostemma pentaphyllum* mixture in high-fat emulsion- and vitamin D3-induced atherosclerotic rats. *J Chin Med Assoc*. 2018;81:398–408.
31. Han J, Gao W, Su D, Liu Y. Gypenoside inhibits RANKL-induced osteoclastogenesis by regulating NF-kappaB, AKT, and MAPK signaling pathways. *J Cell Biochem*. 2018;119:7310–7318.
32. Hong M, Cai Z, Song L, et al. *Gynostemma pentaphyllum* attenuates the progression of nonalcoholic fatty liver disease in mice: a biomedical investigation integrated with in silico assay. *Evid Based Complement Alternat Med*. 2018;2018:8384631.
33. Huang TH, Tran VH, Roufogalis BD, Li Y. Gypenoside XLIX, a naturally occurring PPAR-alpha activator, inhibits cytokine-induced vascular cell adhesion molecule-1 expression and activity in human endothelial cells. *Eur J Pharmacol*. 2007;565:158–165.
34. Li HH, Tyburski JB, Wang YW, et al. Modulation of fatty acid and bile acid metabolism by peroxisome proliferator-activated receptor alpha protects against alcoholic liver disease. *Alcohol Clin Exp Res*. 2014;38:1520–1531.
35. Zhao R, Zhou H, Su SB. A critical role for interleukin-1beta in the progression of autoimmune diseases. *Int Immunopharmacol*. 2013;17:658–669.
36. Wiersinga WM, Prummel MF. Pathogenesis of Graves' ophthalmopathy–current understanding. *J Clin Endocrinol Metab*. 2001;86:501–503.
37. Yoon JS, Lee HJ, Chae MK, Lee EJ. Autophagy is involved in the initiation and progression of Graves' orbitopathy. *Thyroid*. 2015;25:445–454.
38. Shu DY, Lovicu FJ. Myofibroblast transdifferentiation: the dark force in ocular wound healing and fibrosis. *Prog Retin Eye Res*. 2017;60:44–65.
39. Brown KD, Shah MH, Liu GS, et al. Transforming growth factor beta1-induced NADPH oxidase-4 expression and fibrotic response in conjunctival fibroblasts. *Invest Ophthalmol Vis Sci*. 2017;58:3011–3017.
40. Garrett Q, Khaw PT, Blalock TD, et al. Involvement of CTGF in TGF-beta1-stimulation of myofibroblast differentiation and collagen matrix contraction in the presence of mechanical stress. *Invest Ophthalmol Vis Sci*. 2004;45:1109–1116.
41. Huang C, Wang H, Pan J, et al. Benzalkonium chloride induces subconjunctival fibrosis through the COX-2-modulated activation of a TGF-beta1/Smad3 signaling pathway. *Invest Ophthalmol Vis Sci*. 2014;55:8111–8122.
42. Tan J, Tong BD, Wu YJ, Xiong W. MicroRNA-29 mediates TGFbeta1-induced extracellular matrix synthesis by targeting wnt/beta-catenin pathway in human orbital fibroblasts. *Int J Clin Exp Pathol*. 2014;7:7571–7577.
43. Dolcet X, Llobet D, Pallares J, Matias-Guiu X. NF-kB in development and progression of human cancer. *Virchows Arch*. 2005;446:475–482.
44. Macias MJ, Martin-Malpartida P, Massague J. Structural determinants of Smad function in TGF-beta signaling. *Trends Biochem Sci*. 2015;40:296–308.
45. Midgley AC, Rogers M, Hallett MB, et al. Transforming growth factor-beta1 (TGF-beta1)-stimulated fibroblast to myofibroblast differentiation is mediated by hyaluronan (HA)-facilitated epidermal growth factor receptor (EGFR) and CD44 co-localization in lipid rafts. *J Biol Chem*. 2013;288:14824–14838.
46. Wang Y, Rouabhia M, Lavertu D, Zhang Z. Pulsed electrical stimulation modulates fibroblasts' behaviour through

Investigative Ophthalmology & Visual Science

the Smad signalling pathway. *J Tissue Eng Regen Med*. 2017;11:1110–1121.

47. Cheng TC, Lu JF, Wang JS, et al. Antiproliferation effect and apoptosis mechanism of prostate cancer cell PC-3 by flavonoids and saponins prepared from *Gynostemma pentaphyllum*. *J Agric Food Chem*. 2011;59:11319–11329.
48. Tanner MA, Bu X, Steimle JA, Myers PR. The direct release of nitric oxide by gypenosides derived from the herb *Gynostemma pentaphyllum*. *Nitric Oxide*. 1999;3:359–365.
49. Huang TH, Razmovski-Naumovski V, Salam NK, et al. A novel LXR-alpha activator identified from the natural product *Gynostemma pentaphyllum*. *Biochem Pharmacol*. 2005;70:1298–1308.
50. Li L, Jiao L, Lau BH. Protective effect of gypenosides against oxidative stress in phagocytes, vascular endothelial cells and liver microsomes. *Cancer Biother*. 1993;8:263–272.
51. Galgoczi E, Jeney F, Gazdag A, et al. Cell density-dependent stimulation of PAI-1 and hyaluronan synthesis by TGF-beta in orbital fibroblasts. *J Endocrinol*. 2016;229:187–196.

Investigative Ophthalmology & Visual Science